32nd Annual International Conference of the IEEE EMBS
Buenos Aires, Argentina, August 31 - September 4, 2010

Multispectral Transillumination Imaging of Skin Lesions for Oxygenated and Deoxygenated Hemoglobin Measurement

Brian D'Alessandro, Atam P. Dhawan

Department of Electrical and Computer Engineering,
New Jersey Institute of Technology, Newark, NJ

Abstract—**The early detection of melanoma is critical for patient survival. One of the indentifying features of new malignancy is increased blood flow to the lesion. Multispectral transillumination using the Nevoscope has been demonstrated to be an effective tool for imaging the sub-surface vascular architecture of skin lesions. Using multispectral images obtained from this tool in the visible and near-infrared range, as well as the relative difference in spectral absorption due to oxyhemoglobin and deoxyhemoglobin, we propose an empirical method to estimate the blood flow volume within a skin lesion. From the images, estimates of the distribution of both Hb and HbO_2 are calculated along with a ratiometric feature describing the relative oxygen saturation level in the blood. We validate our proposed method through the imaging of a skin phantom with embedded capillaries which can be filled with either an artificial Hb or HbO_2 liquid. Our near-IR, multispectral computations nicely differentiate the Hb filled phantom versus the HbO_2 filled phantom, demonstrating that these chromophores can be successfully separated and individually characterized for use in estimating the relative oxygen saturation of skin tissue.**

I. Introduction

SKIN cancer is the most common form of cancer in the United States. Of the 2.5 million new cancer cases expected to be diagnosed in 2009, 1 million of those will be skin cancer. Most types of skin cancer are highly curable, but the deadliest form, melanoma, is expected to result in over 68,000 new diagnoses and over 8,000 deaths this year. However, the survival rate for melanoma, when it is detected early, is around 99% [2]. Clearly, the early detection and diagnosis of melanoma is crucial to treating the malignancy and preventing death.

The problem is that early detection of melanoma is difficult. As a result, much effort is being put into the evaluation of noninvasive optical imaging techniques as a way to detect and analyze the morphological changes associated with tumorigenesis, thereby improving patient diagnosis accuracy with minimal need for invasive and time consuming biopsy procedures. Since primary information is typically obtained from surface lighting, the deeper pigmentation structure is often overcome by the surface light reflection and thus obscures important information regarding the extent of the malignancy. Deeper subsurface information, such as subcutaneous pigmentation and indications of increased blood flow (angiogenesis) are critical factors in early melanoma detection.

II. Procedures And Methods

To obtain this critical subsurface information, the Nevoscope has been developed as a multispectral transillumination light microscopy method for imaging skin lesions [3, 4]. The Nevoscope uses a fiber optic illumination ring to transmit light directly into the skin at an angle so that the light is focused underneath the surface behind the lesion. Light that enters the skin through this ring undergoes multiple internal reflection, scattering, and absorption events depending on the chromophores encountered. The light eventually gets diffused across the layers of the skin and backscattered light photon energy forms a transilluminated image of the skin and skin lesion. Figure 1 shows the difference between surface illumination and transillumination imaging methods.

Longer wavelengths of visible light penetrate deeper into tissue than shorter wavelengths. Consequently, multispectral transillumination imaging provides a way to obtain depth resolved information on subsurface skin features. The aggregation of these multispectral images produces more information than white light imaging alone, and when used in conjunction with a computer aided processing algorithm, can help to make a more intelligent diagnosis.

Our objective in this paper is to obtain information about one particular subsurface skin feature: the blood flow volume within a lesion. Angiogenesis is a key factor in the development of cancerous tissue. Thus, the oxyhemoglobin (HbO_2) and deoxyhemoglobin (Hb) distribution within the lesion, as well as in the surrounding areas, can be of immense value to assess the initiation and proliferation of malignancy.

To this end, we develop an algorithmic method to post-process and combine skin images from transillumination by the Nevoscope at near-infrared and infrared wavelengths in order to obtain an estimate of the HbO_2 and Hb distribution in the skin, as well as a ratiometric measurement descriptive of the relative oxygen saturation level of the blood volume.

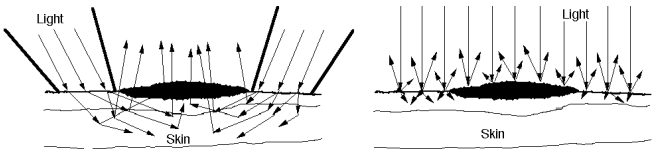

Figure 1. Left: Transillumination Imaging,
Right: Surface Reflectance Imaging

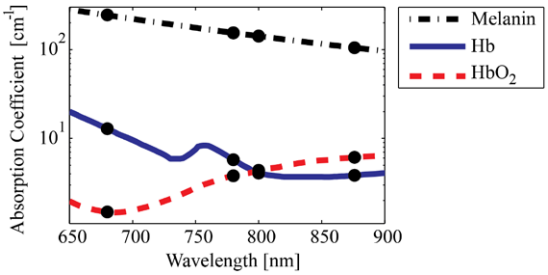

Figure 2. Absorption spectra of Melanin, Hb, and HbO_2 [1]. Black dots pinpoint values at 680, 780, 800, and 875 nm.

We validate our proposed method through the use of a skin phantom to which we can add artificial Hb or HbO_2 beneath the surface of the phantom to provide the appropriate absorption effects in our transillumination images. In doing so, we demonstrate the feasibility of unmixing multiple chromophore distributions using transillumination in skin tissue.

III. Multi-Chromophore Measurement

Absorption of HbO_2 and Hb varies depending on wavelength (Figure 2). As wavelength increases in the 680 nm to 800 nm range, absorption of Hb decreases while absorption of HbO_2 increases. Thus, by comparing the localized absorption difference between two or more wavelength ranges, we should obtain a measure how much spectral distortion is caused by blood absorption. Of course, because of the diffusive nature of light in tissue, the actual absorption coefficient is difficult to obtain. A precise quantitative result is confounded by scattering as well as by the absorption of other components such as melanin.

Any attempt at a description of chromophore distribution and its effects on backscattered light must begin with a model of light transport in tissue. Diffusion theory has been used as an approximation of the radiative transport equations to describe light propagation in a turbid medium. The diffusion equation for the absorption and scattering of light is defined for position $\vec{r}$ and time t by:

$$\frac{\partial\Phi(\vec{r},t)}{c\partial(t)}+\mu_a\Phi(\vec{r},t)-\nabla\cdot\left[\frac{\nabla\Phi(\vec{r},t)}{3(\mu_a+\mu_s(1-g))}\right]=S(\vec{r},t) \quad (1)$$

where Φ is fluence rate, μ_a and μ_s are absorption and scattering coefficients, g is the anisotropy factor, and S is an isotropic light source. Solutions to the above diffusion equation generally show an exponential attenuation of light in a medium for a given depth l, with the wavelength dependent absorption and scattering coefficients as $\mu_a(\lambda)$ and $\mu_s(\lambda)$. In our model, we assume the minimum penetration depth level among all selected wavelengths for ratiometric analysis. Furthermore, to simplify the problem of estimating absorption, we assume μ_s to be constant over the selected spectral bandwidth of light. Considering these constraints, for a specific wavelength λ, the diffused light remittance intensity A_λ at a particular point is roughly proportional to $\mu_a(\lambda)$ at that same point. The value A_λ can be thought of as the grey level value of one imaged pixel. With the Nevoscope imaging geometry, the entire image thus represents the total spatial map of backscattered diffuse reflectance.

Absorption due to the background skin can be eliminated from the calculations through division by an image of the background without any other extra chromophores present:

$$\hat{A}_\lambda=1-\frac{A_\lambda}{A_\lambda^{background}} \quad (2)$$

This essentially results in $\hat{A}_\lambda$ representing the percent difference in absorption due to the added chromophores relative to the background.

Although the spatial dependence of the absorption coefficients cannot be *exactly* known, $\hat{A}_\lambda$ is related to the absorption of each chromophore present in the medium. We can assume that these absorptions are linearly combined for imaging. For example, the major chromophores in the skin are melanin, HbO_2, and Hb. The total normalized absorption is thus a function of the unknown amount of melanin [*Mel*], oxyhemoglobin [HbO_2], and deoxyhemoglobin [*Hb*]:

$$\hat{A}_\lambda=[Mel]\mu_{Mel}^\lambda+[HbO_2]\mu_{HbO_2}^\lambda+[Hb]\mu_{Hb}^\lambda \quad (3)$$

where μ_{Mel}^λ, $\mu_{HbO_2}^\lambda$, and μ_{Hb}^λ are the wavelength dependent absorption coefficients of melanin, HbO_2, and Hb.

With three unknowns, we need to utilize three equations, or three imaging wavelengths, to solve for the amounts of each chromophore. Our normalized chromophore expressions using imaging at 680, 780, and 800 nm are thus:

$$\hat{A}_{680}=[Mel]\mu_{Mel}^{680}+[HbO_2]\mu_{HbO_2}^{680}+[Hb]\mu_{Hb}^{680} \quad (4)$$

$$\hat{A}_{780}=[Mel]\mu_{Mel}^{780}+[HbO_2]\mu_{HbO_2}^{780}+[Hb]\mu_{Hb}^{780} \quad (5)$$

$$\hat{A}_{800}=[Mel]\mu_{Mel}^{800}+[HbO_2]\mu_{HbO_2}^{800}+[Hb]\mu_{Hb}^{800} \quad (6)$$

Given the imaged pixel values for the three wavelengths as well as the absorption coefficients of melanin, HbO_2 and Hb, the linear system defined by the three equations above can be solved to obtain estimates of [*Mel*], [HbO_2], and [*Hb*], or, the amounts of melanin, oxyhemoglobin, and deoxyhemoglobin present under the area imaged by the pixel.

Once the estimates of [HbO_2] and [*Hb*] are found, we wish to find an estimate of the *total* relative absorption for Hb and HbO_2 across the 100 nm between 680 and 780 nm. To do this, we compute a linear approximation of the area underneath the absorption curve for each chromophore, modified by the amount of that chromophore:

$$\overline{Hb}=\tfrac{1}{2}\left([Hb]\mu_{Hb}^{680}+[Hb]\mu_{Hb}^{780}\right)(100\text{nm}) \quad (7)$$

$$\overline{HbO_2}=\tfrac{1}{2}\left([HbO_2]\mu_{HbO_2}^{680}+[HbO_2]\mu_{HbO_2}^{780}\right)(100\text{nm}) \quad (8)$$

The $\overline{HbO_2}$ estimate itself relates to how much spectral absorption is caused by oxyhemoglobin, and therefore, is a measure of blood oxygen saturation (SO_2). Thus, if we want to visualize SO_2 and its spatial localization we can simply

analyze the $\overline{HbO_2}$ image. Another method of visualization is to compute a ratiometric measurement defining SO_2 relative to the total amount of blood. Total blood is simply $\overline{HbO_2} + \overline{Hb}$, therefore our ratiometric measurement of percent oxygen saturation in the blood is:

$$R = \left(\overline{HbO_2}\right) \Big/ \left(\overline{HbO_2} + \overline{Hb}\right) \quad (9)$$

All of the aforementioned equations are evaluated on a pixel by pixel basis given the acquired images at each wavelength, resulting in 2D solutions for the [HbO_2] and [Hb] estimates, as well as R.

IV. Skin Phantom

The evaluation of our imaging system involves the creation of a skin phantom to form a known physical structure with which we can test and calibrate our image acquisition as well as validate our chromophore and ratiometric features. We have followed the general procedure outlined by Lualdi et al. for the development of a tissue-like phantom which matches the optical properties of skin for the visible and near infrared range using Al_2O_3 particles, cosmetic powder, and silicone [5].

We also embedded five capillary tubes at varying depths within the phantom which can be filled with liquid and reused to simulate the presence of blood in our imaging (Figure 3a). Each tube is 1mm in diameter and is positioned at depths in increments of 0.5 mm (Figure 3b).

We created artificial oxyhemoglobin by mixing hemoglobin powder with water and exposing the solution to air. This resulted in a bright reddish fluid similar in color to oxygenated blood. We deoxygenated this mixture by adding a small amount of yeast [6], which turned the solution a darker, murkier, purple color, typical of venous blood. However, we found that the measured absorption spectrum of these two fluids matched quite closely to the absorption spectrum of red and blue food coloring. As a result, we used the red and blue food coloring for artificial HbO_2 and Hb throughout the rest of our experiments, as these were easier, safer, and less costly to work with.

Once placed in contact with the surface of the skin phantom, the Nevoscope transilluminates the phantom. A camera attached to the Nevoscope images the backscattered diffuse reflectance from the skin phantom and the contents of the capillary tubes. We are thus able to obtain and compare images for phantoms filled with HbO_2 or Hb over varying depths and varying illumination wavelengths.

V. Image Acquisition and Results

Our methods were implemented on transilluminated images of our skin phantom as well as a normal skin lesion. The imaging apparatus consisted of a monochrome Andor Luca CCD camera connected through a 25 mm Fujinon 3CCD lens to a multispectral Nevoscope. The transillumination fiber ring of the Nevoscope was sourced by a Schott KL 2500 LCD light source containing three

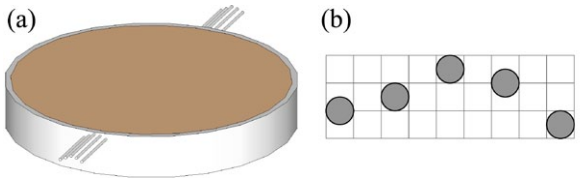

Figure 3. (a) Phantom with capillary tubes. (b) Capillary tube layout (grid is 1 mm x 1 mm).

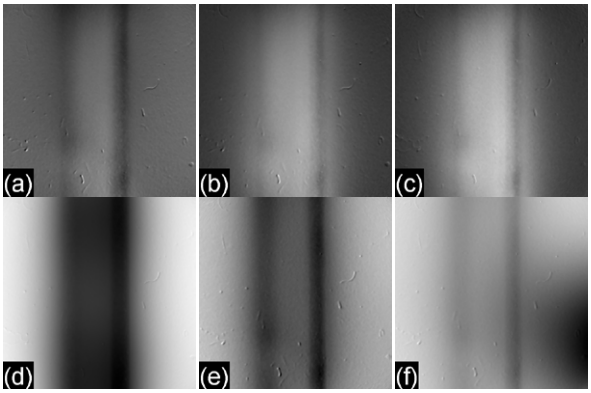

Figure 4. Transilluminated skin phantom images; two capillary tubes filled with artificial HbO_2 at (a) 680 nm (b) 780 nm (c) 800 nm; two capillary tubes filled with artificial Hb at (d) 680 nm (e) 780 nm (f) 800 nm.

Chroma optical filters, 680, 780, and 800 nm. The images were then normalized to correct for the exposure time as well as the relative response curve of the light source and CCD. Images obtained using this camera and lens system have a field of view of approximately 1cm x 1cm. Images were preprocessed with a median filter to eliminate a very minor amount of salt and pepper noise from the CCD.

We used our phantom to obtain multispectral images for two experiments. In the first, the two uppermost capillary tubes were filled with artificial HbO_2; in the second these were filled with artificial Hb. For background normalization, we also imaged the phantom when the tubes were empty. These normalized images are shown for transillumination with 680 nm, 780 nm, and 800 nm light in Figure 4. The left tube is at a depth of 0.5 mm while the right tube is at a depth of 1.0 mm. There are clear differences among the set of six images, owing to the wavelength and chromophore dependant scattering and absorption.

In our phantom, no extra melanin is present, so [Mel] in (4)-(6) is zero. As a result, we only need two imaging wavelengths and two equations to solve the linear system for [HbO_2] and [Hb]:

$$\hat{A}_{680} = [HbO_2]\mu_{HbO_2}^{680} + [Hb]\mu_{Hb}^{680} \quad (10)$$

$$\hat{A}_{780} = [HbO_2]\mu_{HbO_2}^{780} + [Hb]\mu_{Hb}^{780} \quad (11)$$

Using the 680 and 780 nm images, along with (2), (10)-(11), and then (7)-(8), results in the HbO_2 and Hb area

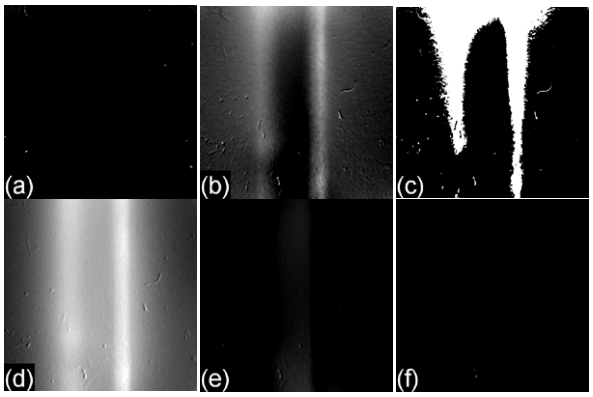

Figure 5. (a) $\overline{Hb}$ estimate for HbO_2 filled phantom. (b) $\overline{HbO_2}$ estimate for HbO_2 filled phantom. (c) *R* estimate for HbO_2 filled phantom. (d) $\overline{Hb}$ estimate for Hb filled phantom. (e) $\overline{HbO_2}$ estimate for Hb filled phantom. (f) *R* estimate for Hb filled phantom.

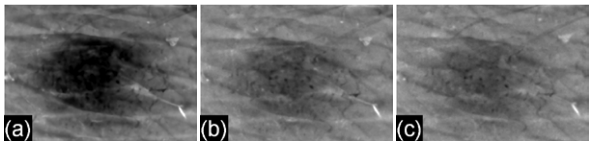

Figure 6. Transilluminated normal skin lesion images at (a) 680nm (b) 780nm (c) 800 nm.

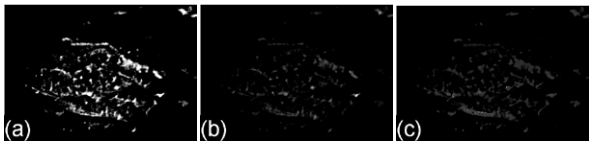

Figure 7. (a) $\overline{Hb}$ estimate, (b) $\overline{HbO_2}$ estimate, and (c) ratiometric image *R* for a normal skin lesion.

estimates shown in Figure 5. Our method very nicely differentiates the two chromophores; for the HbO_2 filled phantom, the $\overline{Hb}$ estimate in (a) is practically zero while the $\overline{HbO_2}$ estimate in (b) clearly highlights the location of HbO_2 within the two tubes. Likewise, for the Hb filled phantom, the $\overline{HbO_2}$ estimate in (e) is very low, while the $\overline{Hb}$ estimate in (d) is high for the tube locations. In both cases, the right tube (which is closest to the surface) is more clearly defined while the deeper left tube appears blurred due to the diffuse nature of the phantom and poor depth resolution of tissue optical illumination.

Before obtaining the ratiometric image using (9), we first threshold and segment out areas of high intensity from the $\overline{HbO_2}$ image (i.e. locations of high SO_2) and then perform the ratiometric calculation only on the pixels within the region of interest. For the high intensity areas of SO_2 in the HbO_2 filled phantom, the ratiometric values are around one, correctly indicating that 100% of the artificial blood in that case is HbO_2 (Figure 5c). On the other hand, 0% of the Hb filled phantom is HbO_2 resulting in values of zero throughout the *R* image (Figure 5f).

We also test our method on the multispectral images (Figure 6) of a normal skin lesion. Since melanin is a major chromophore in skin lesions, we use the three wavelengths to solve (4)-(6). The solutions for $\overline{Hb}$, $\overline{HbO_2}$, and *R* are given in Figure 7. The lesion is benign, so blood volume surrounding the lesion is small relative to melanin content, especially compared with what would exist in an abnormal lesion. Validation of real skin lesions can only be done with clinical trials, which we intend to perform based on the good results and successful validation of our phantom.

VI. Discussion

In this paper, we have presented a method of estimating the oxy- and deoxy-hemoglobin content and relative oxygen saturation level in the skin. We validate our techniques through the use of a skin-like tissue phantom with embedded capillary tubes. When we imaged the phantom with two tubes filled with artificial HbO_2, our method was able to determine that based on the multispectral images at 680 and 780 nm, HbO_2 was in fact present in the phantom whereas Hb was not. Similarly, in the reverse case where the two tubes were filled with Hb, no HbO_2 was detected and the Hb estimate image showed high Hb concentration in the spots where the tubes were located. Since the absorption spectrum difference between these two chromophores is sufficiently large, we obtain good differentiation in separating out images of each chromophore. Our goal is to find the relative oxygen saturation level of a skin lesion, and with our ratiometric calculations, our phantom has demonstrated this is possible. We plan to extend our method to clinical imaging of skin lesions to correlate Hb, HbO_2, and the relative oxygen saturation ratio to the grade of dysplasia for early detection and classification of skin cancers including malignant melanomas.

References

[1] S. Prahl. 1999, Optical Absorption of Hemoglobin Available: http://omlc.ogi.edu/spectra/hemoglobin/

[2] *Skin Cancer Facts*. Available: http://www.skincancer.org/skin-cancer-facts/ (2009, Accessed March 26, 2010).

[3] A. P. Dhawan, "Apparatus and method for skin lesion examination," US Patent Number 5,146,923, September 15, 1992.

[4] A. P. Dhawan, B. D'Alessandro, S. Patwardhan, and N. Mullani, "Multispectral Optical Imaging of Skin-Lesions for Detection of Malignant Melanomas," in *IEEE EMBS Conference of the IEEE Engineering in Medicine and Biology Society*, 2009.

[5] M. Lualdi, A. Colombo, B. Farina, S. Tomatis, and R. Marchesini, "A phantom with tissue-like optical properties in the visible and near infrared for use in photomedicine," *Lasers in Surgery and Medicine,* vol. 28, pp. 237-243, 2001.

[6] J. E. Bender, K. Vishwanath, L. K. Moore, J. Q. Brown, V. Chang, G. M. Palmer, and N. Ramanujam, "A robust monte carlo model for the extraction of biological absorption and scattering in vivo," *IEEE Transactions on Biomedical Engineering,* vol. 56, pp. 960-968, 2009.